

Supporting Information for

Doping engineering of the flexible polyaniline electrochromic material through H₂SO₄-HClO₄ multiple acids for the radiation regulation in snow environment

Gaoping Xu, Leipeng Zhang, Bo Wang, Zichen Ren, Xi Chen, Shuliang Dou, Feifei Ren, Hang Wei, Xiaobai Li*, Yao Li*

Center for Composite Materials and Structure, Harbin Institute of Technology, Harbin 150001, PR China

*Corresponding Author.

E-mail address: lixiaobai2008@126.com, yaoli@hit.edu.cn

Table of content

<u>General methods</u>	S3
<u>Table S1.</u>	S4
<u>Fig. S1</u>	S5
<u>Fig. S2</u>	S5
<u>Fig. S3</u>	S6
<u>Fig. S4</u>	S6
<u>Fig. S5</u>	S7
<u>Fig. S6</u>	S7
<u>Fig. S7</u>	S8
<u>Fig. S8</u>	S8
<u>References</u>	S8

General methods

The value of ε can be calculated by weighting $(1 - R(\lambda))$ (namely spectral emittance) with the black body spectrum for a particular wavelength and integrating over the entire measured wavelength range according to the following two equations:

$$B_{(\lambda)} = \frac{c_1 \lambda^{-5}}{\exp[c_2 / (\lambda T)] - 1} \quad (1)$$

$$\varepsilon = \frac{\int_{\lambda_{\min}}^{\lambda_{\max}} (1 - R(\lambda)) B(\lambda) d\lambda}{\int_{\lambda_{\min}}^{\lambda_{\max}} B(\lambda) d\lambda} \quad (2)$$

where c_1 is the first radiation constant ($3.7418 \times 108 \text{ W } \mu\text{m}^4 \text{ m}^{-2}$), c_2 is the second radiation constant ($1.4388 \times 10^4 \text{ } \mu\text{m K}$), λ is the wavelength, and T is the temperature.

The route for the assembly of the device: The PANI films doped with H_2SO_4 - HClO_4 on the Au substrate are used as the front and back electrodes, and nanoporous polyethylene (PE) is devoted to a protective layer. The (poly vinylidenefluoride-hexafluoro propylene) copolymer containing electrolyte is used as the electrolyte film. After each layer is assembled together, the device is firmly compressed using a roll-to-roll mode at 190°C .

Cyclic durability testing of polyaniline: After the initial test of emissivity, the device was scanned for cyclic voltammetry. After 10 cycles of scanning, the emissivity was tested *in situ*.

The simulation of the device: The thermal properties of the device were simulated by finite element method, implemented in the commercial software ANSYS. In all cases, steady-state thermal model was used to record the temperature at which the pipe reaches the steady state of heat transfer. In addition, the transient thermal module was also used to record the temperature of the pipe at different times. For simplicity, the heat dissipation from the device to the air is only mediated by natural convection and radiation. And, the pipe is set to have different heat flow.

The thermal regulation performance test of the device: The apparatus is composed of a heater and insulation materials blocking the conductive and convective heat exchange with surroundings. The EC device was placed on the apparatus. Subsequently, a thermal imager was used to record the surface temperature of the EC device.

Table S1. Comparison for the performances of the EC device with the reported devices.

EC devices	Working materials	Doping acids	Tunable spectral range	Response time	$\Delta\epsilon$ at 8-14 μm	Flexible	UV reflectivity	Working voltage	Ref.
Device 1	Polyaniline	$\text{H}_2\text{SO}_4\text{-HClO}_4$	2.5 μm-25 μm	13-14 s	0.47	Yes	>80%	0.5 V/-0.4 V	This work
Device 2	Polyaniline/WO ₃	Camphorsulfonic acid	5 μm -20 μm	9 s	0.41	NO	<10%	0.45V/-0.2V	1
Device 3	Polyaniline/poly(diphenyl amine)	Poly(styrene sulfonate)	2.5 μm -18 μm	2 s	0.39	Not reported	<10%	0 V/-1.1 V	2
Device 4	Polyaniline/poly(diphenyl amine)	Poly(styrene sulfonate)	2.5 μm -25 μm	2 s	<0.4	Yes	<20%	0.8 V/-1.1 V	3
Device 5	Polyaniline	Poly(styrene sulfonate)	2.5 μm -25 μm	Not reported	0.35	Yes	<5%	0.3 V/-0.9 V	4
Device 6	Ppoly-O-anisidine	H_2SO_4	2.5 μm -25 μm	Not reported	<0.3	NO	<5%	0.2 V/-1.1 V	5
Device 7	Polyaniline	H_2SO_4	2.5 μm -25 μm	Not reported	<0.3	NO	Not reported	1.0V/-0.6V	6
Device 8	Polyaniline	H_2SO_4	2.5 μm -25 μm	<5 s	<0.2	NO	Not reported	0.55 V/-0.25V	7
Device 9	Polyaniline	Dodecylbenzene sulfonate acid	2.5 μm -25 μm	Not reported	<0.4	Yes	Not reported	0.45 V/-0.25 V	8
Device 9	Polyaniline	Dodecylbenzene sulfonate acid	2.5 μm -25 μm	Not reported	<0.3	NO	<20%	0.85 V/-0.25 V	9
Device 10	Polyaniline	Dodecylbenzene sulfonate acid	2.5 μm -25 μm	>15 s	<0.4	YES	<20%	0.2 V/-1.2V	10
Device 11	Polyaniline	H_2SO_4	2.5 μm -25 μm	Not reported	0.39	YES	Not reported	Not reported	11

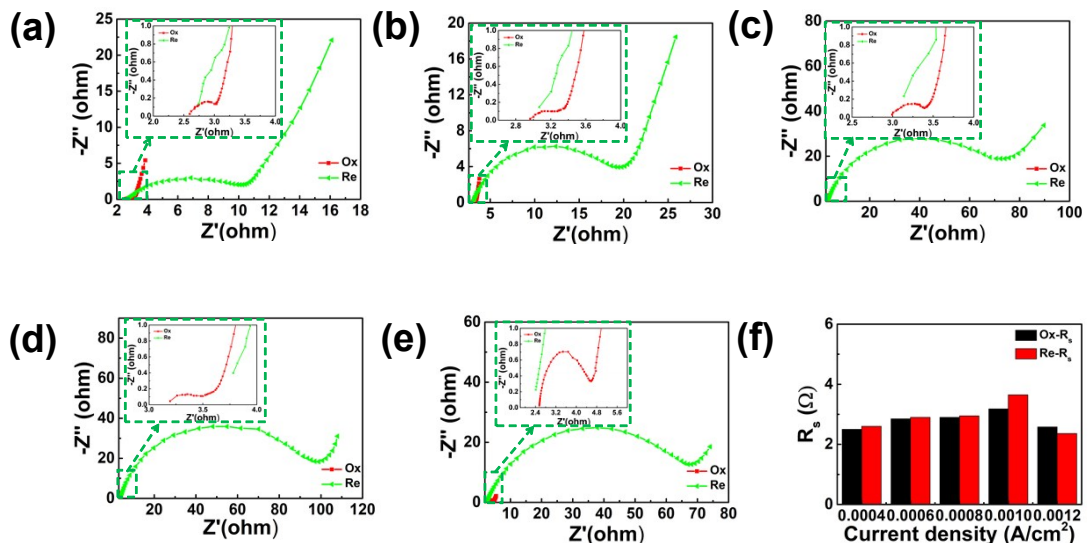


Fig. S1. EIS of the PANI films at different polymerization current densities. (a) 0.0001 A/cm². (b) 0.00015 A/cm². (c) 0.0002 A/cm². (d) 0.00025 A/cm². (e) 0.0003 A/cm². (f) R_s of the PANI films at different polymerization current densities.

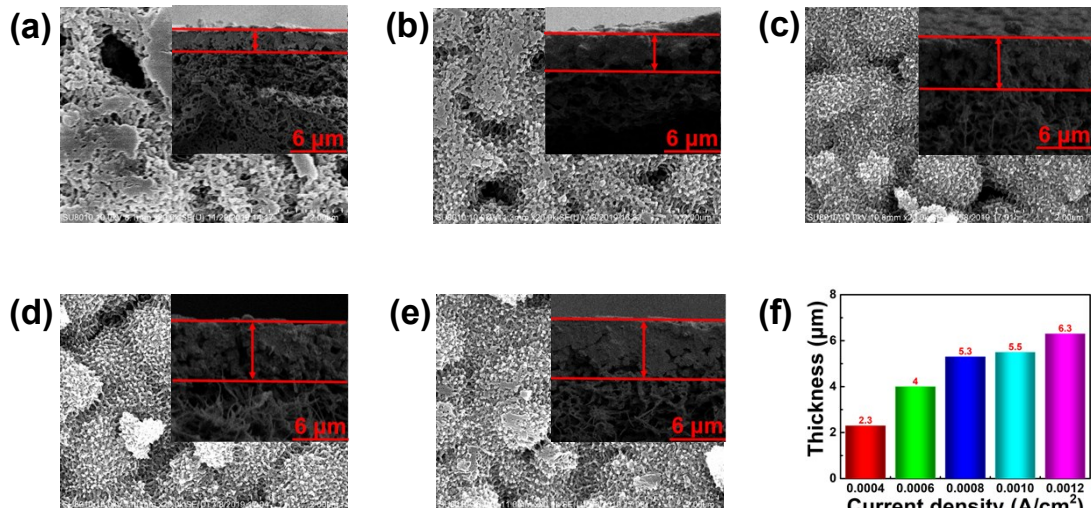


Fig. S2. SEM images of PANI films at different polymerization current densities. (a) 0.0001 A/cm². (b) 0.00015 A/cm². (c) 0.0002 A/cm². (d) 0.00025 A/cm². (e) 0.0003 A/cm². (f) The thickness of the PANI films at different polymerization current densities. Inset: SEM cross-section images of PANI films at different polymerization current densities.

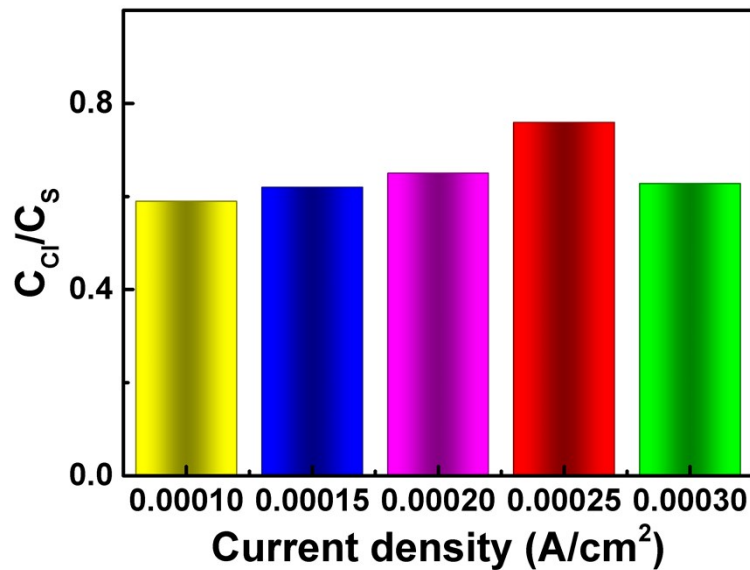


Fig. S3. The ratio of chlorine element to sulfur element at different polymerization current densities.

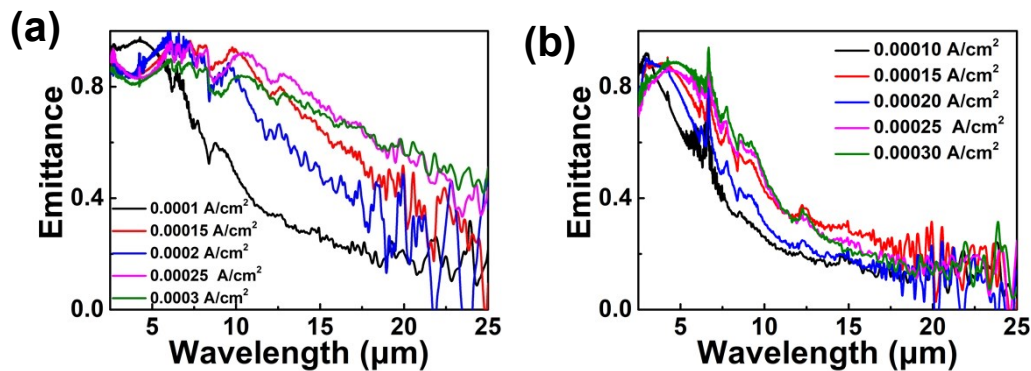


Fig. S4. (a) Emittance curves of PANI films prepared at different polymerization current densities at potential of 0.4 V. (b) Emittance curves of PANI films prepared at different polymerization current densities at potential of -0.5 V.

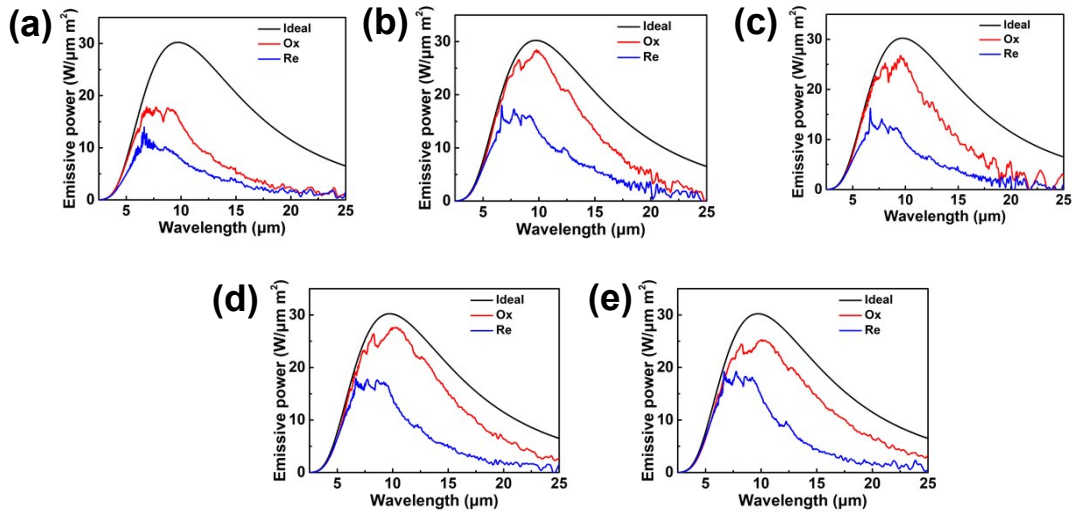


Fig. S5. The emissive power curves of PANI films prepared at different polymerization current densities at potential of 0.4 V and -0.5 V. (a) 0.0001 A/cm². (b) 0.00015 A/cm². (c) 0.0002 A/cm². (d) 0.00025 A/cm². (e) 0.0003 A/cm².

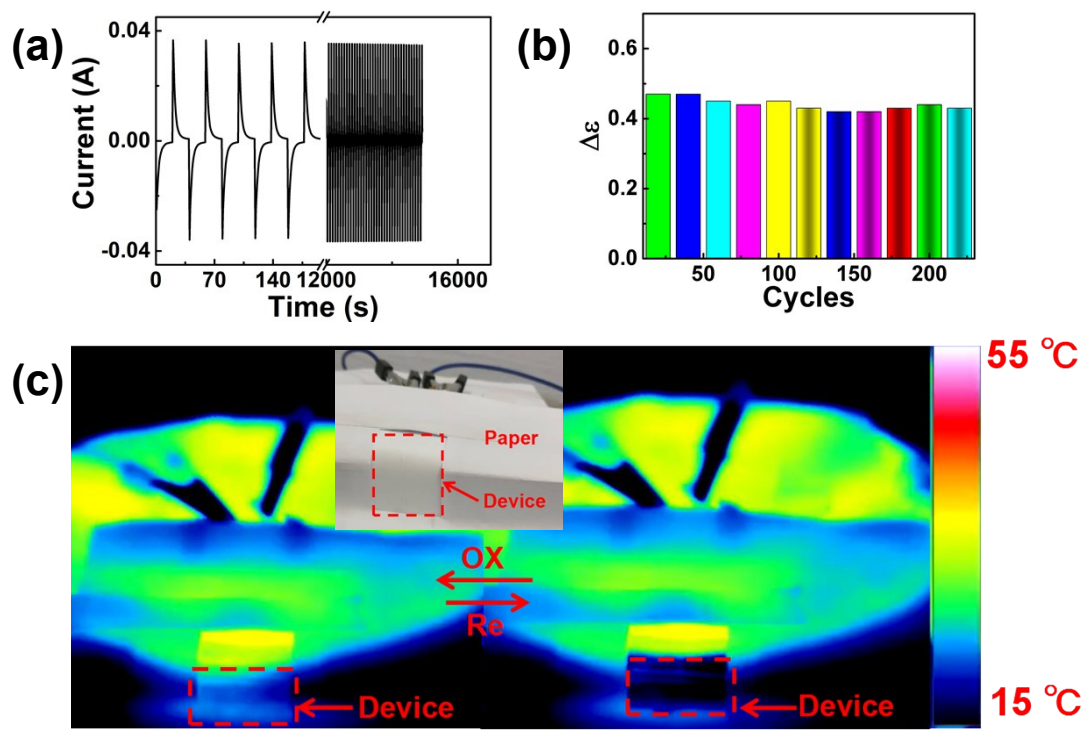


Fig. S6. (a) The I-t curve of the device under applied voltage. (b) Cyclic durability of the device. (c) IR thermal images of the EC device under bending state on the Al plate.

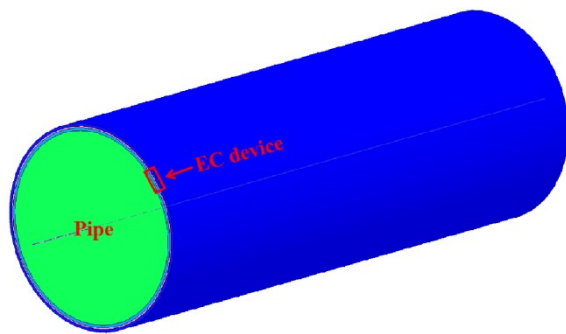


Fig. S7. Schematic of the heat transfer of the EC device in the finite element simulation.

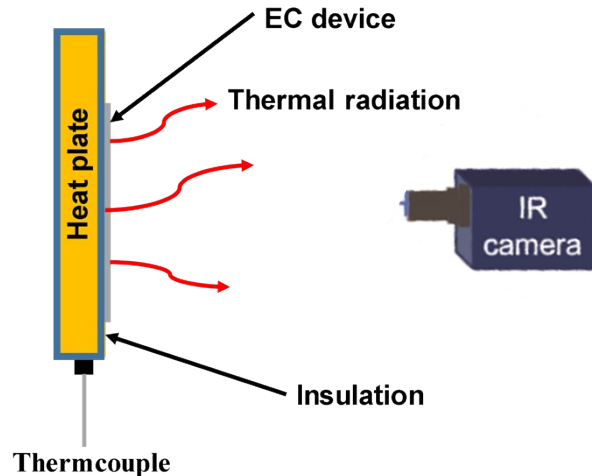


Fig. S8. The schematic setup for thermal regulation of the device.

References:

1. P. Topart and P. Hourquebie, *Thin Solid Films*, 1999, **352**, 243-248.
2. P. Chandrasekhar, G. C. Birur, P. Stevens, S. Rawal, E. A. Pierson, and K. L. Miller, *Synth. Met.*, 2001, **119**, 293-294.
3. P. Chandrasekhar, B. J. Zay, G. C. Birur, S. Rawal, E. A. Pierson, L. Kauder and S. Theodore, *Adv. Funct. Mater.* 2002, **12**, 95-103.
4. P. Chandrasekhar, B. J. Zay, T. Mcqueeney, G. C. Birur, V. Sitaram, R. Menon, M. Coviello and R.L. Elsenbaumer, *Synth. Met.*, 2005, **155**, 623-627.
5. L. Tu, C. Jia, X. Weng and L. Deng, *Synth. Met.*, 2011, **161**, 2045-2048.
6. S. Wu, C. Jia, X. Fu, X. Weng, J. Zhang and L. Deng, *Electrochim. Acta*, 2013, **88**, 322-329.
7. Y. Tian, S. Dou, X. Zhang, L. Zhang, L. Wang, J. Zhao, X. Zhao and Y. Li,

Synth. Met., 2017, **232**, 111-116.

8. Y. Tian, X. Zhang, S. Dou, L. Zhang, H. Zhang, H. Lv, L. Wang, J. Zhao and Y. Li, *Sol. Energy Mater. Sol. Cells*, 2017, **170**, 120-126.
9. L. Zhang, D. Li, X. Li, B. Wang, G. Xu, X. Zhao, G. Xia, A. Gavrilyuk, J. Zhao and Y. Li, *Dyes Pigm.*, 2019, **170**, 107570.
10. X. Li, L. Zhang, B. Wang, G. Xu, S. Yu, M. Pan, S. Dou, Y. Li and J. Zhao, *Electrochim. Acta*, 2020, **332**.
11. F. Lu, P. Tan and Y. Han, *J. Appl. Polym. Sci.*, 2020, e49622.